LCLS-II-HE IMPACT Tracking (May 2019)

Ji Qiang, LBNL

LCLS-II-HE 20-06

6/24/2020

SLAC

1 Introduction

In this study, the LCLS-II-HE beam dynamics simulation using the IMPACT code starts with an initial distribution at the exit of the LCLS-II injector. This is based on the assumption that there is no upgrade of the injector design in the HE project. The computational model in the IMPACT code includes exact transfer map through a drift, linear transfer map for hard edge quadrupole with energy dependence, 5^{th} order transfer map through dipole, linear transfer matrix through RF superconducting cavity, thin lens kick model for sextupole, self-consistent 3D space-charge effects, 1D steady state and transient coherent synchrotron radiation (CSR) effects, incoherent synchrotron radiation (ISR) effects through a bending magnet, longitudinal structure and resistive wall wakefields, and uncorrelated energy increase from an analytical intrabeam scattering (IBS) model. We have used real number of electrons in the simulation to capture the initial shot-noise of the beam and 64x64x2048 computational grid points to calculate the space-charge effects. The accelerator lattice is based on the MAD input file of Nov. 27, 2018.

2 Beam Dynamics Simulation through LCLS-II-HE Linac with 100pC Charge

The initial longitudinal phase space particle distribution and the current profile for accelerator beam dynamics optimization and simulation are shown in Fig. x.1. The initial peak current is about 12 A and the initial relative rms energy spread is 0.07%.

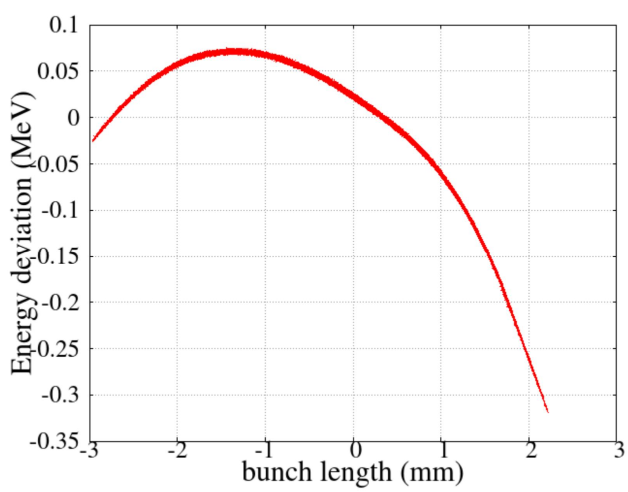

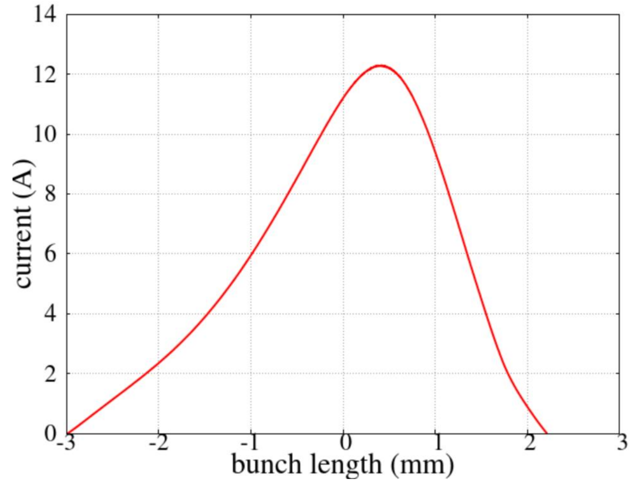

Fig. x.1: Longitudinal phase distribution (left) and current profile (right) of the beam at the exit of the LCLS-II injector (100pC).

Using the above initial distribution, we optimized 10 control parameters in the LCLS-II-HE linear accelerator (linac) using a variable population with external storage multi-objective parallel differential evolution algorithm. The two objective functions in the optimization are the rms energy spread and the fraction of charge inside a given bunch length window at the entrance of the undulator. The 10 control parameters used in the optimization are the linac 1 RF cavity amplitude and phase, the 3rd harmonic linearizer RF cavity amplitude and phase, the BC1 bending angle, the linac 2 RF cavity amplitude and phase, the BC2 bending angle, and the linac 3a RF cavity amplitude and phase. Fig. x.2 shows the Pareto front of the final rms energy spread and fraction of charge within a given bunch length window after the optimization.

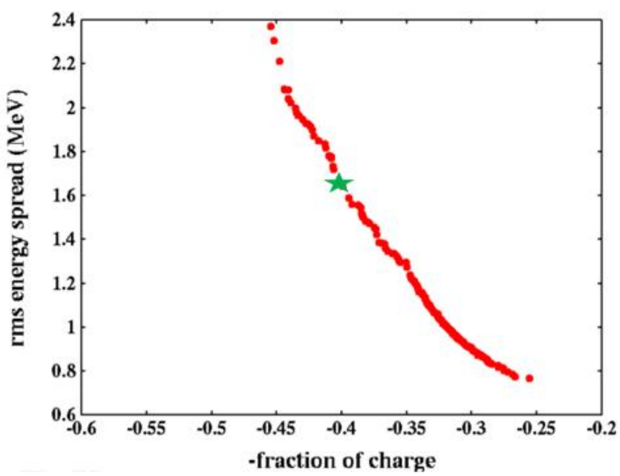

Fig. x.2: Pareto front of the final rms energy spread and fraction of charge after optimization.

It is seen that the larger fraction of charge within the window, the larger rms energy spread would be. From this Pareto front, we select an optimal solution (green star in the figure) with reasonable energy spread and peak current. The settings of the accelerator for this optimal solution are given as follows:

- Laser heater induced energy spread: 6 keV
- L1 Eamp = 15.76 MV/m

- L1 Phase = -17.9 deg.
- HL Eamp = 10.5 MV/m (57.95 MV)
- HL Phase = -159.83 deg.
- BC1 R56 = -0.0513m
- E_{bc1} = 294.56 MeV
- Relative rms energy spread 1.3%
- L2 Eamp = 17.49 MV/m
- L2 Phase = -21.3 deg.
- BC2 R56 = -0.0639 m
- E_{bc2} = 1917.98 MeV
- L3a Eamp = 17.48MV/m
- L3a Phase = 1.9 deg.
- L3b Eamp = 17.45MV/m
- L3b Phase = 5.1 deg.
- L4 Eamp = 19.55MV/m
- L4 Phase = 3.83 deg.
- E_{final} = 8043.55 MeV

After the longitudinal beam dynamics optimization, using the above settings of the optimal solution, we retuned some quadrupole settings in the accelerator including space-charge effects in order to rematch to the designed Twiss parameters. Those retuned quadrupole parameters are given as follows:

- QCM01 k value: 0.33883
- Q0H1- 4 k values: -6.5456, 6.1093, 2.0498, -5.6968
- Q0H5 -8 k values: -7.7217, 2.2553, 7.7818, -8.2955
- QHD01- 4 k values: -8.8069, 6.4481, -8.6698, 6.8272
- QC001- 4 k values: 5.8635, -1.4093, -5.0265, 3.1598
- QC101-105 k values: -0.3386, 0.0, 1.8479, -0.2543, -1.9838

Using those lattice parameter settings and the MAD Nov. 28 inputs, we carried out start-to-end beam dynamics simulation of the entire beam delivery system using the real number of 100pC electrons and 64x64x2048 grid points. Fig. x. 3 shows the beam kinetic energy evolution through the accelerator beam delivery system. The electron beam is accelerated to about 295 MeV before entering the first bunch compressor BC1. After BC1, the beam is accelerated in linac 2 to about 1918 GeV before entering the second bunch compressor BC2. After BC2, the beam is further accelerated in linac 3 and linac 4 to final 8 GeV.

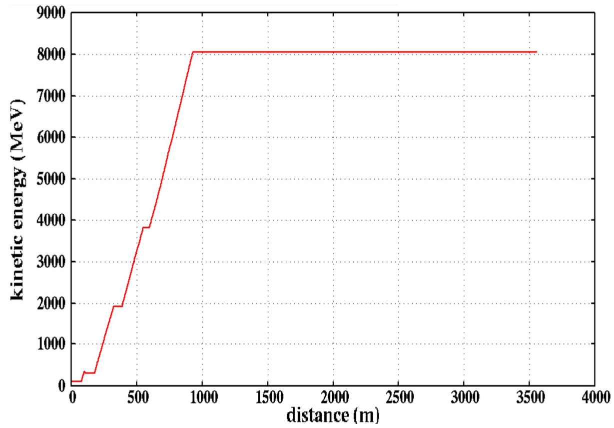

Fig. x. 3: Electron beam kinetic energy evolution through the accelerator beam delivery system.

Fig. x. 4 shows the longitudinal phase space and current profile after the BC1. The beam is compressed only by a factor of about three and maintains a good linear longitudinal phase space after the BC1. Small modulation is seen in the current profile. Fig. x. 5 shows the longitudinal phase space and current profile

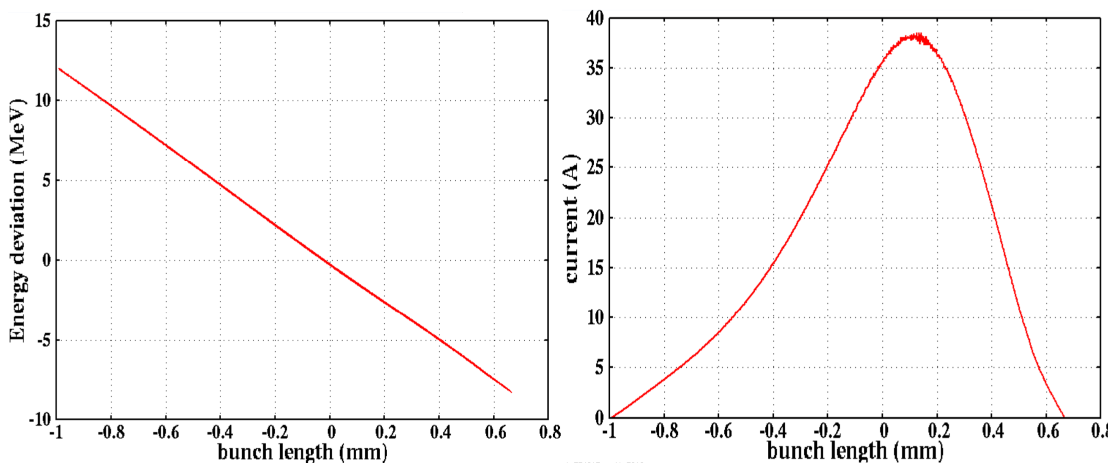

Fig. x.4: Longitudinal phase distribution (left) and current profile (right) of the beam after BC1.

after the BC2. There is about a factor of 40 compressions after BC2. The current in the core of the beam is beyond 1.4 kA with a spike beyond 2.5 kA near the head of the beam. Some particles in the head of the distribution folds in after BC2. Fig. x.6 shows the final longitudinal phase space and current at the entrance of the undulator. The chirped longitudinal phase space becomes flat at the entrance of the undulator from the collective effects (mostly from the resistive wall wakefield effects).

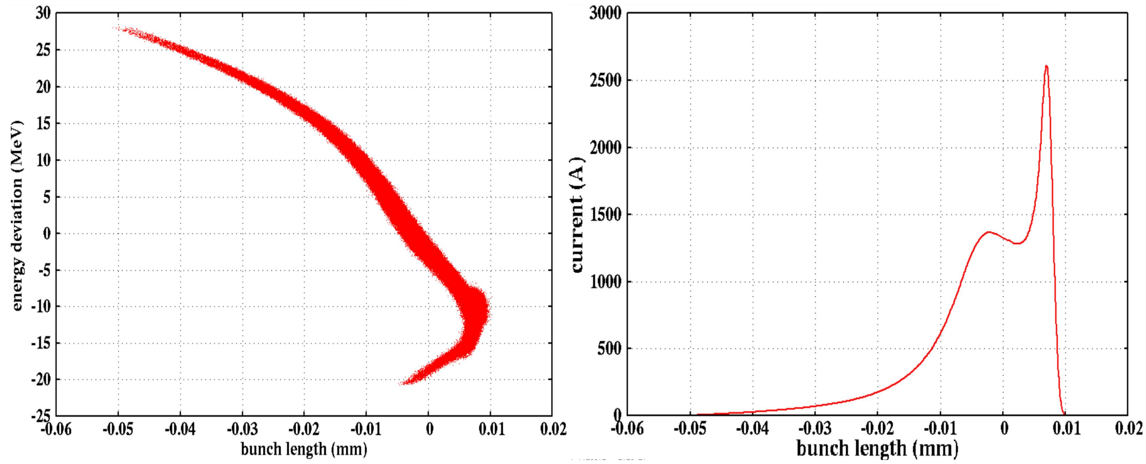

Fig. x.5: Longitudinal phase distribution (left) and current profile (right) of the beam after BC2.

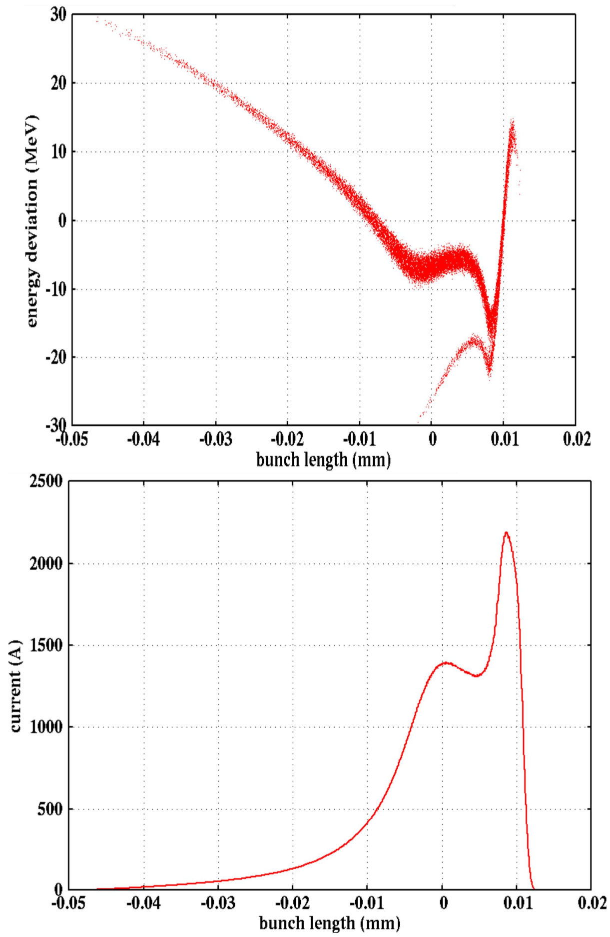

Fig. x.6: Longitudinal phase distribution (left) and current profile (right) of the beam at the entrance of the undulator.

The current profile in Fig. x.6 includes the fold-in particles from the head particles. Fig. x.7 shows the longitudinal phase space, current profile, and uncorrelated energy spread at the entrance of the undulator after removing the long tail and the head of particle distribution. The peak current in the core of the distribution is beyond 1.3 kA. There is about 12 um flat beam region in the core of the phase space distribution. The uncorrelated energy spread in this region is about 1 MeV.

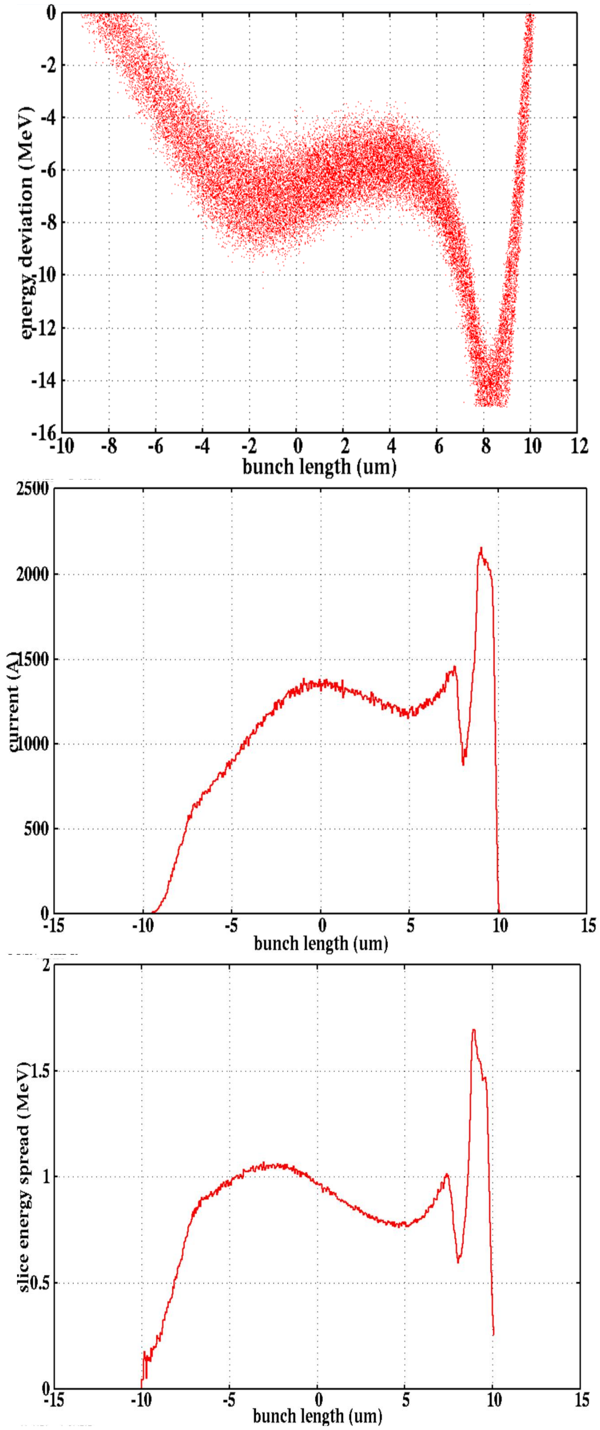

Fig. x.7: Longitudinal phase distribution (left), current profile (right), uncorrelated energy spread of the beam at the entrance of the undulator after removing the fold-in and long tail particles.

As shown in the above list, some quadrupoles are retuned including space-charge effects to improve the matching of the transverse beam size through the accelerator. Fig. x.8 shows the transverse rms sizes evolution through the HE accelerator beam delivery system. It is seen that the beam is reasonably matched through the accelerator. Fig. x.9 shows the transverse rms projected emittance evolution through the accelerator. The major projected emittance growth is after the BC2 due to the CSR effects. The final projected emittance is below 0.5 um in both x and y planes. Fig. x.10 shows the final slice emittance distribution across the beam at the entrance to the undulator. Inside the core part of the beam, both horizontal and vertical slice emittances are below 0.3 um.

Table 1 gives a summary of the final electron beam parameters from the IMPACT simulation through the accelerator beam delivery system. The averaged current inside the core is beyond 1.2 kA, with about 900 keV averaged uncorrelated energy spread, less than 0.5 um projected emittances, and below 0.3 um slice emittances. This beam will be used for FEL radiation performance study.

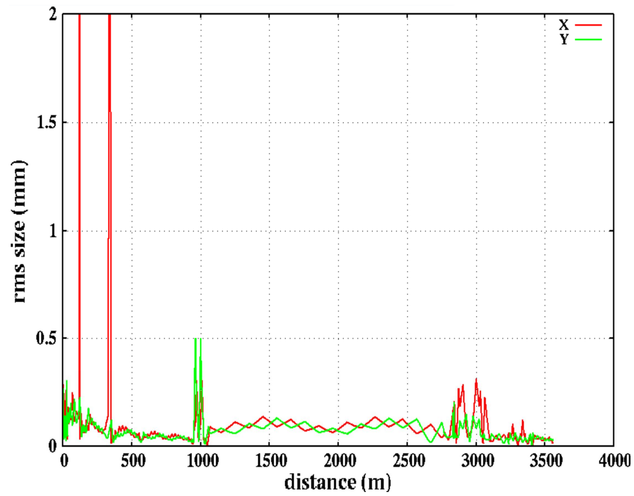

Fig. x.8: Transverse RMS beam size evolution through the beam delivery system.

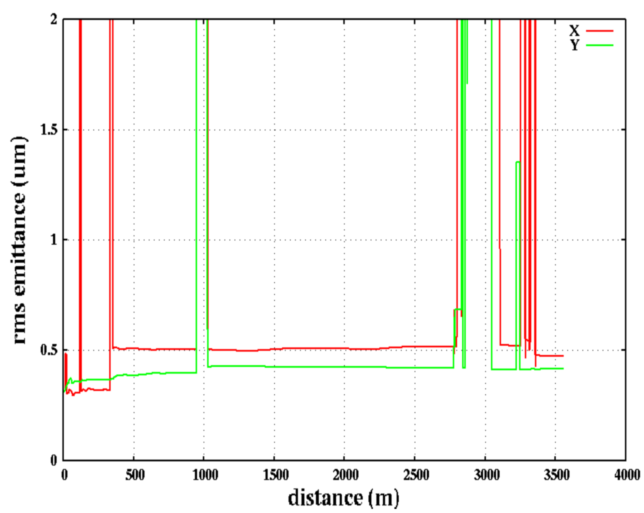

Fig. x.9: Transverse RMS emittance evolution through the beam delivery system.

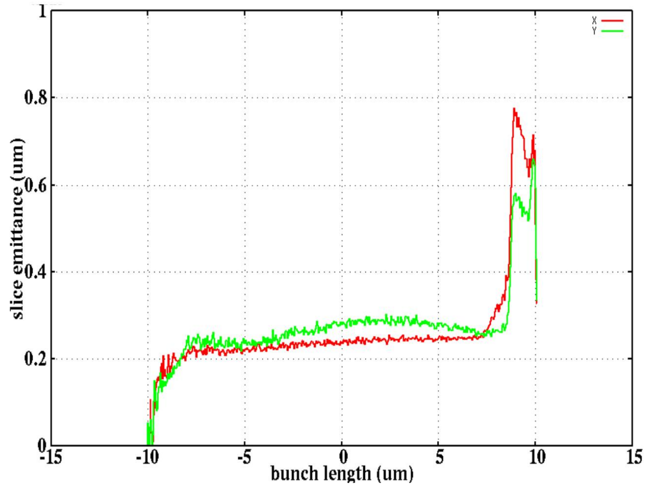

Fig. x.10: Transverse slice emittance profile of the beam at the entrance of undulator.

Table x.1: Summary of final beam parameters of 100pC at the entrance to the undulator

IMPACT Studies	**I_peak** (A)	σ_E (keV)	**Proj.** ε_x / ε_y (mm-mrad)	**Slice** ε_x / ε_y (mm-mrad)
100 pC	1238	920	0.47 / 0.42	0.24 / 0.27

3 Beam Dynamics Simulation through LCLS-II-HE Linac with 20pC Charge:

The IMPACT simulation of the 20pC charge through the LCLS-II-HE accelerator beam delivery system also started with an initial distribution at the exit of the injector since there is no change in the original LCLS-II injector for the HE upgrade.

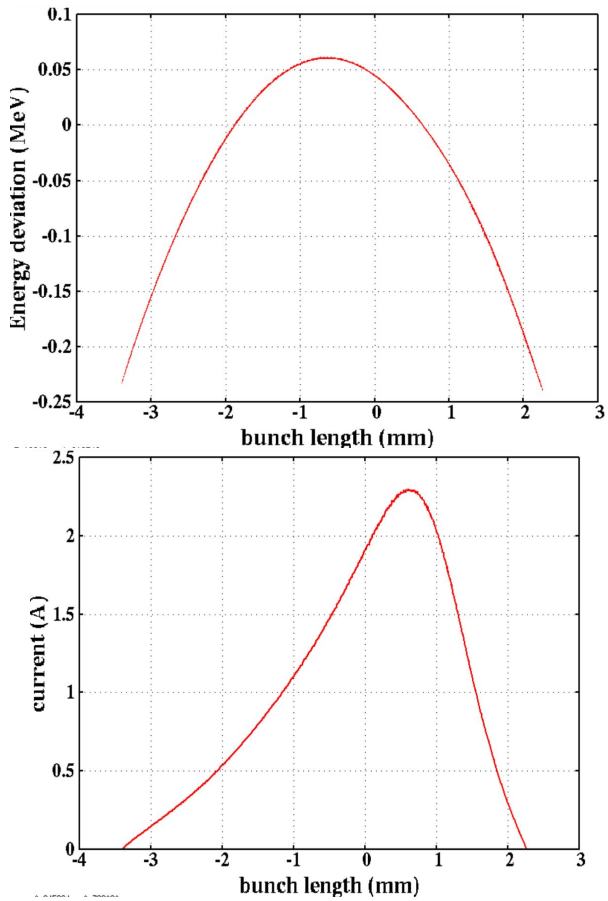

Fig. x.11: Longitudinal phase distribution (left) and current profile (right) of the beam at the exit of the LCLS-II injector (20pC).

Fig. x.11 shows the longitudinal phase space distribution and current profile at the exit of the injector. The peak current is slightly below 2.5 A with a small relative energy spread of 0.03%. Using this initial distribution, we did multi-objective longitudinal beam dynamics optimization for the 20pC beam following the same way as we did for the 100pC case. Fig. x.12 shows the Pareto front of the final rms energy spread and negative fraction of charge within a given bunch length window after the optimization. The larger the fraction of charge inside the window, the larger rms energy spread it has.

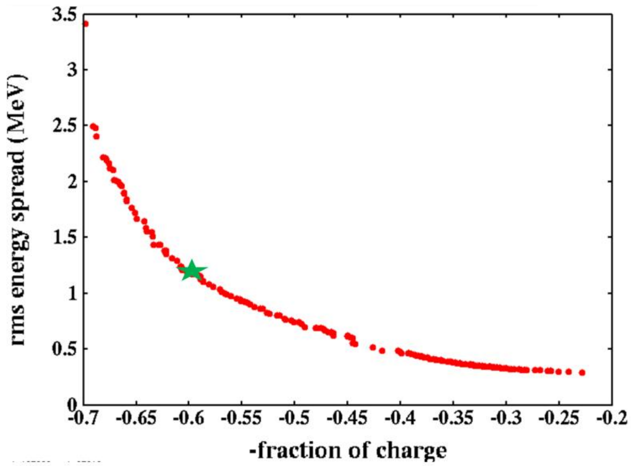

Fig. x.12: Pareto front of the final rms energy spread and fraction of charge after optimization (20pC).

We selected one optimal solution (green star) from the Pareto front with reasonable rms energy spread and peak current. The settings of the accelerator for this optimal solution are given as follows:

- Laser heater induced energy spread: 2.5 keV
- L1 Eamp = 15.2 MV/m
- L1 Phase = -22.4 deg.
- HL Eamp = 12.81 MV/m (70.7 MV)
- HL Phase = -160.6 deg.
- BC1 R56 = -0.0566m
- E_{bc1} = 267.0 MeV
- Relative rms energy spread 2.1%
- L2 Eamp = 17.0 MV/m
- L2 Phase = -0.7 deg.
- BC2 R56 = -0.00383 m
- E_{bc2} = 1956.31 MeV
- L3a Eamp = 17.1 MV/m
- L3a Phase = 5.73 deg.
- L3b Eamp = 17.45MV/m
- L3b Phase = 5.1 deg.
- L4 Eamp = 19.55MV/m
- L4 Phase = 3.83 deg.
- E_{final} = 8040.7 MeV

Using the above settings of the optimal solution, we retuned some quadrupole settings in the accelerator including space-charge effects in order to rematch to the designed Twiss parameters. Those retuned quadrupole parameters are given as follows:

- QCM01 k value: -1.7098
- Q0H1- 4 k values: -7.9998, 7.5705, -2.6868, 6.2449
- Q0H5 -8 k values: -7.8854, 2.9136, 7.4889, -8.1569
- QHD01- 4 k values: -8.7616, 6.4074, -8.6660, 7.0391

- QC001- 4 k values: 1.4557, 4.8839, -6.2124, 2.1589
- QC101-105 k values: -0.1538, 0.0, 1.8624, -0.2731, -1.8763

Using those lattice parameter settings and the MAD Nov. 28 inputs, we carried out start-to-end beam dynamics simulation of the entire beam delivery system using the real number of 20pC electrons and 64x64x2048 grid points. Fig. x. 13 shows the beam kinetic energy evolution through the accelerator beam delivery system. The electron beam is accelerated to about 267 MeV in linac 1 before entering the first bunch compressor BC1. After BC1, the beam is accelerated in linac 2 to about 1956 GeV before entering the second bunch compressor BC2. After BC2, the beam is further accelerated in linac 3 and linac 4 to final 8 GeV.

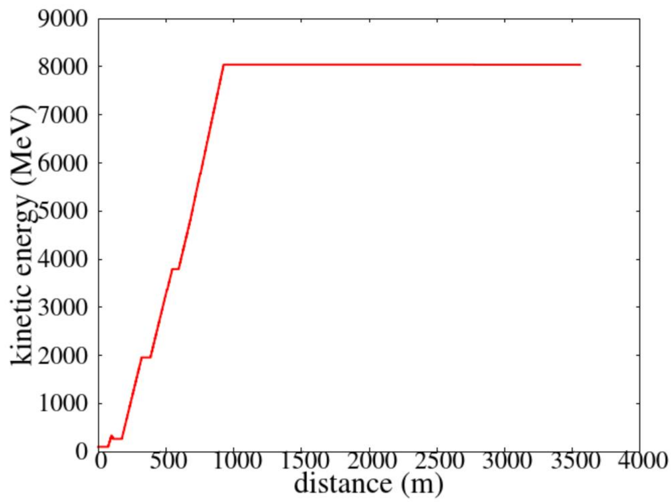

Fig. x. 13: Electron beam kinetic energy evolution through the accelerator beam delivery system (20pC).

Fig. x. 14 shows the longitudinal phase space and current profile after the BC1. The beam is compressed by a factor of about 70 and maintains a reasonable linear longitudinal phase space after the BC1. Small modulation is seen in the current profile. Fig. x. 15 shows the longitudinal phase space and current profile after the BC2. There are about a factor of 4 compressions after BC2. The peak current inside the core of the beam is beyond 500 A with a spike over 600 A around the head and the tail of the distribution. Fig. x.16 shows the final longitudinal phase space, current profile, the uncorrelated energy spread at the entrance of the undulator. The chirped longitudinal phase space is flatten out at the entrance of the undulator from the collective effects. The peak current in the core of the distribution is beyond 500 A. There is about 7 um flat beam region in the core of the distribution. The uncorrelated energy spread in the core is about 700 keV.

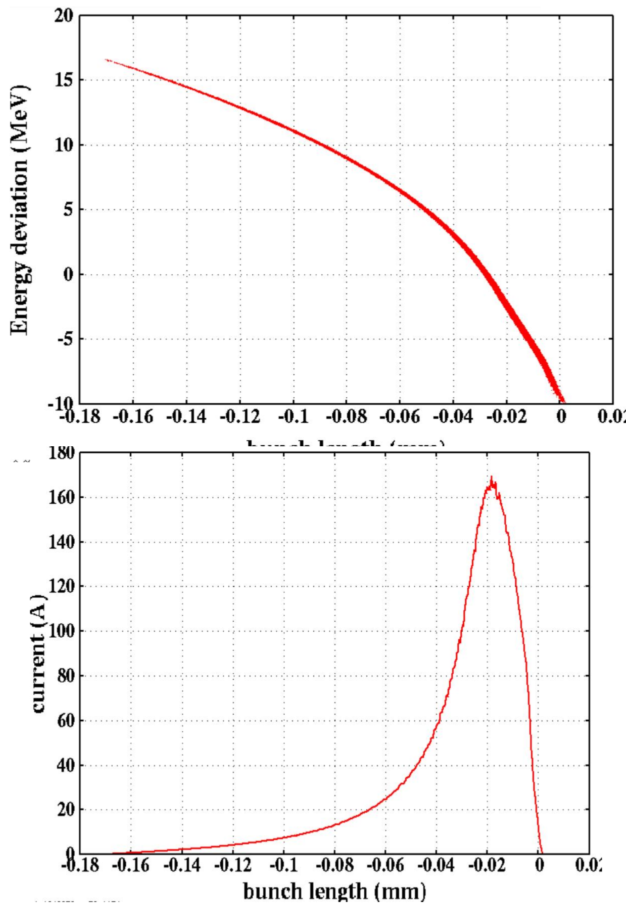

Fig. x.14: Longitudinal phase distribution (left) and current profile (right) of the beam after BC1 (20pC).

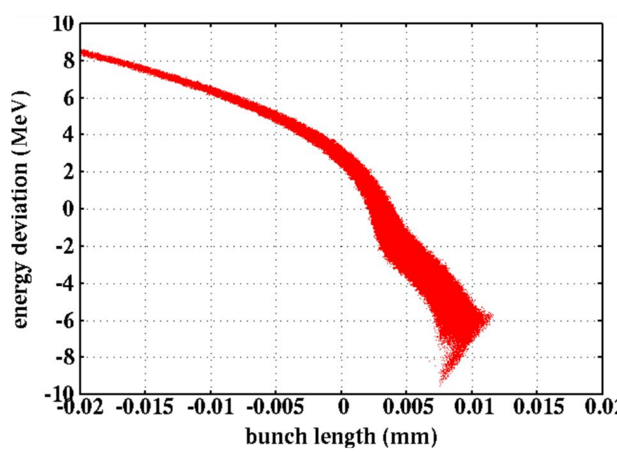

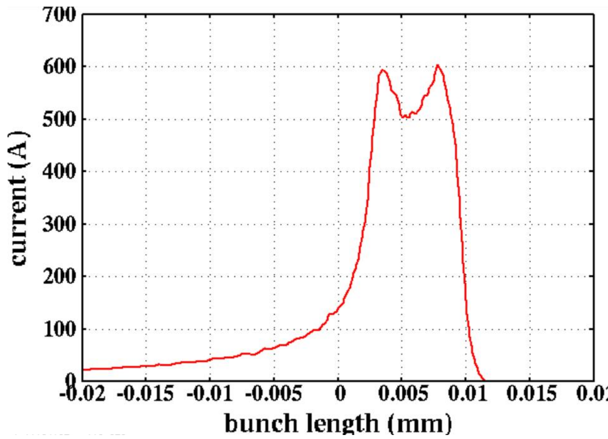

Fig. x.15: Longitudinal phase distribution (left) and current profile (right) of the beam after BC2 (20pC).

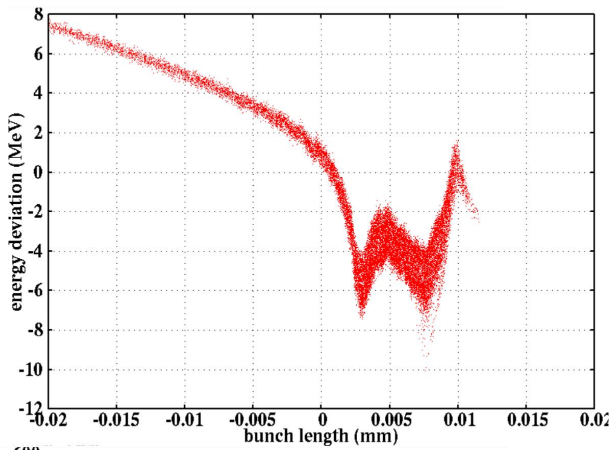

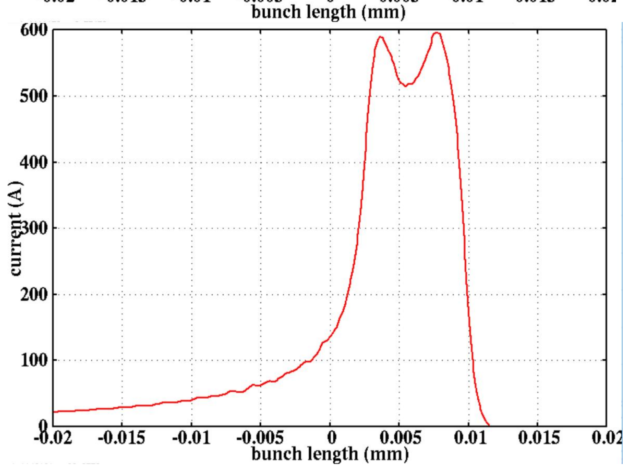

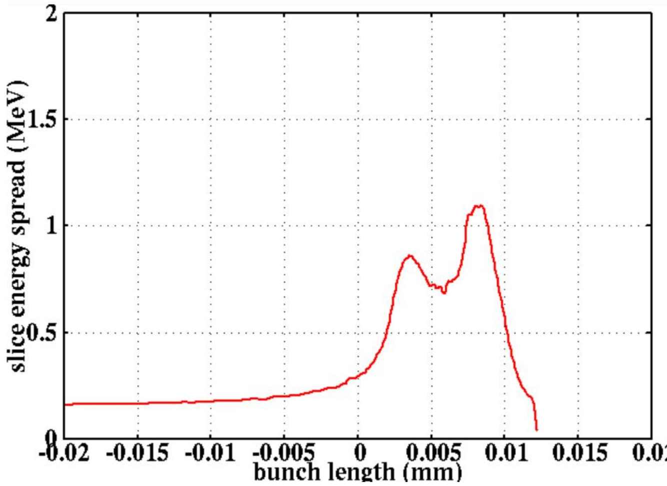

Fig. x.16: Longitudinal phase distribution (left), current profile (right), and uncorrelated energy spread (bottom) of the beam at the entrance of the undulator (20pC).

As shown in the above list, some quadrupoles are retuned including space-charge effects to improve the matching of the beam transverse size through the accelerator. Fig. x.17 shows the transverse rms sizes evolution through the accelerator beam delivery system. It is seen that the beam reasonably matched through the accelerator except inside the long transport beam line. Fig. x.18 shows the transverse rms projected emittance evolution through the accelerator. The major projected emittance growth is after the BC1 due to the strong CSR effects. The final projected emittances are about 0.2 um in both x and y planes. Fig. x.19 shows the final slice emittance distribution across the beam at the entrance of the undulator. In the core part of the beam, both horizontal and vertical slice emittances are below 0.2 um.

Table 2 gives a summary of the final electron beam parameters from the IMPACT simulation through the LCLS-II-HE accelerator beam delivery system using 20pC charge. The averaged current inside the core is beyond 500 A, with about 800 keV averaged uncorrelated energy spread, about 0.2 um projected emittances, and below 0.2 um slice emittances. This beam will be used for further FEL radiation performance study.

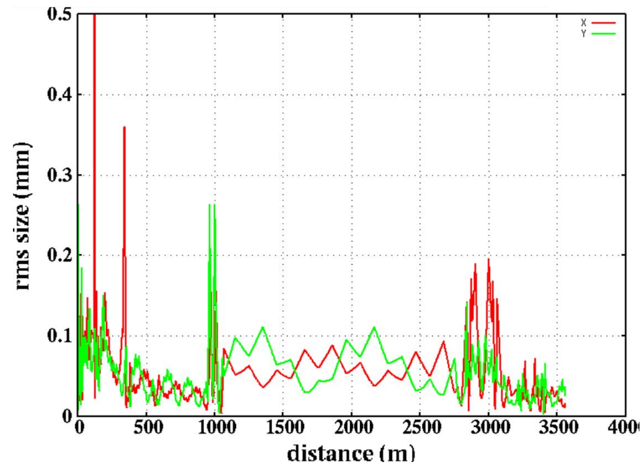

Fig. x.17: Transverse RMS beam size evolution through the beam delivery system (20pC).

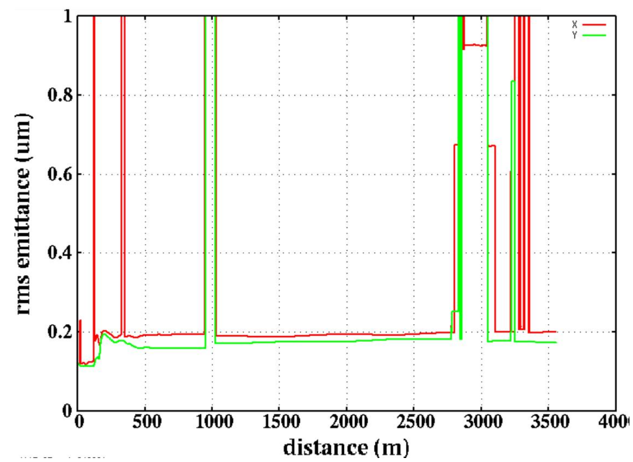

Fig. x.18: Transverse RMS emittance evolution through the beam delivery system (20pC).

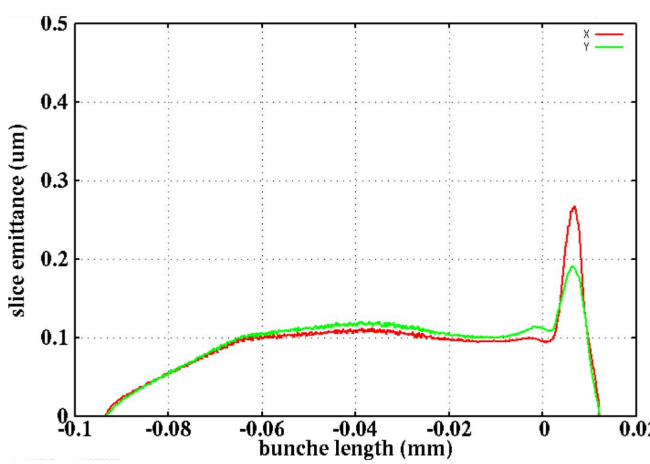

Fig. x.19: Transverse slice emittance profile of the beam at the entrance of undulator (20pC).

Table x.2: Summary of final beam parameters of 20pC at the entrance to the undulator

IMPACT Studies	**I_peak** (A)	σ_E (keV)	**Proj.** ε_x / ε_y (mm-mrad)	**Slice** ε_x / ε_y (mm-mrad)
20 pC	522	840	0.2 / 0.18	0.19 / 0.16